Romanian Reports in Physics **70**, XYZ (2018)

THE ADOMIAN DECOMPOSITION METHOD FOR THE SLIP FLOW AND HEAT TRANSFER OF NANOFLUIDS OVER A STRETCHING/SHRINKING SHEET

HUDA O. BAKODAH [1,*] , ABDELHALIM EBAID [2]
[1] Department of Mathematics, Faculty of Science-Al Faisaliah Campus, King Abdulaziz University, Jeddah, Saudi Arabia
[2] Department of Mathematics, Faculty of Science, University of Tabuk, P.O. Box 741, Tabuk 71491, Saudi Arabia
[*] Corresponding author: E-mail: *hbakodah@kau.edu.sa*

Received October 26, 2017

Abstract. In this paper, the problem of heat transfer of the boundary layer nanofluid flow over a stretching and a shrinking sheet has been investigated in the presence of the suction and the slip parameters. In the case of stretching sheet, the current exact results for the heat transfer rate (in the absence of some parameters) have been compared with the numerical ones in the literature, where some differences are found. In the presence of the slip parameter and no suction, the present results by using a few components of Adomian's series agree with those of the homotopy analysis method in the literature. In the case of shrinking sheet, the exact dual solution is obtained in a special case, while the approximate dual solution has been obtained in the general case by Adomian's method. In addition, the effects of the suction, the slip, the Brownian motion parameter, and the thermophoresis parameters on the dual velocity, the dual temperature, and the dual nano-particle concentration have been discussed through graphs.

Key words: Nanofluid, shrinking sheet, dual solution, Adomian decomposition method.

1. INTRODUCTION

To solve initial and boundary value problems for ordinary, partial and integral equations, the Adomian decomposition method (ADM) [1] is an effective tool as demonstrated by several researchers [2–11]. For a boundary value problem, the series solution obtained by the ADM usually converges to the available exact solution. Also, if the exact solution is not available such as the case of the Thomas-Fermi equation, Ebaid [7] showed that the sequence of approximate solutions converge to a certain function. However, some difficulties arise when the ADM is used to solve boundary value problems in infinite domain, where the conditions at infinity cannot be directly implemented to construct the recurrence scheme. Boundary value problems in infinite domain are frequently arising in various scientific models and recently in the field of boundary layer nanofluid flows [12–16].

In the literature [17–23], many authors were directed either to the Padé technique or the semi-analytical methods to overcome these difficulties.

Computationally, the Padé technique needs a great effort to obtain accurate results. An approach has been recently proposed by Ebaid *et al*. [21] to implement the ADM to solve the boundary value problems in infinite domain. Their approach was based on obtaining the solution of the governing system in closed form and then using the ADM to approximate the physical quantities of interest. The main observation on the paper [21] was that it dealt with a certain kind of boundary conditions that gives a unique solution in the case of stretching sheet. In the case of shrinking sheet, a dual solution exists for the velocity, the temperature, and the nano-particle concentration. In this regard, the ADM has not previously applied to treat such kinds of problems and therefore the present results have not reported in the literature, to the best of our knowledge. Morover, the ADM can be also extended to cover many scientific models [24–36].

In this work, the ADM is developed to solve a new type of boundary-layer flow and heat transfer of nanofluids over both a stretching/shrinking sheet under the effects of the suction and the slip parameters. The proposed problem is an extension of [23] given by the following set of nonlinear ordinary differential equations :

$$f'''(\eta) + f(\eta) f''(\eta) - \left(f'(\eta)\right)^2 = 0, \tag{1}$$

$$\frac{1}{Pr}\theta''(\eta) + f(\eta)\theta'(\eta) + Nb\,\phi'(\eta)\theta'(\eta) + Nt\left(\theta'(\eta)\right)^2 = 0, \tag{2}$$

$$\phi''(\eta) + Lef(\eta)\phi'(\eta) + \frac{Nt}{Nb}\theta''(\eta) = 0, \tag{3}$$

subject to the boundary conditions:

$$f(0) = s, \quad f'(0) = \pm 1 + \lambda f''(0), \quad \theta(0) = 1, \quad \phi(0) = 1, \tag{4}$$

$$f'(\infty) = 0, \quad \theta(\infty) = 0, \quad \phi(\infty) = 0, \tag{5}$$

where the positive and negative signs refer to the case of the stretching sheet and the shrinking sheet, respectively. Pr, Le, Nb, Nt, s, and λ are respectively, Prandtl number, Lewis number, Brownian motion parameter, thermophoresis parameter, suction parameter, and partial slip parameter. The exact solution of Eq. (1) with the boundary conditions in (4-5) is given as

$$f(\eta) = a + b\,e^{-\beta\eta}, \quad a = s \pm \frac{1}{\lambda\beta^2 + \beta}, \quad b = \mp\frac{1}{\lambda\beta^2 + \beta}, \tag{6}$$

where β is the positive real root for the following cubic equation

$$\lambda\beta^3 + (1 - \lambda s)\beta^2 - s\beta \mp 1 = 0. \tag{7}$$

Hence, Eqs. (2) and (3) become

$$\theta''(\eta) + Pr\left[a + b\,e^{-\beta\eta} + Nb\,\phi'(\eta)\right]\theta'(\eta) + PrNt\left[\theta'(\eta)\right]^2 = 0, \tag{8}$$

$$\phi''(\eta) + Le\left(a + b\,e^{-\beta\eta}\right)\phi'(\eta) + \frac{Nt}{Nb}\theta''(\eta) = 0. \tag{9}$$

2. CLOSED FORM SOLUTION

On solving Eq. (8) for $\theta'(\eta)$, we have

$$\theta'(\eta) = \frac{e^{Pr[-a\eta+\frac{b}{\beta}e^{-\beta\eta}-Nb\,\phi(\eta)]}}{e^{Pr(\frac{b}{\beta}-Nb)}/\theta'(0)+PrNt\int_0^\eta e^{Pr[-a\sigma+\frac{b}{\beta}e^{-\beta\sigma}-Nb\,\phi(\sigma)]}d\sigma}, \tag{10}$$

which can be integrated once with respect to η to get

$$\theta(\eta) = 1+\frac{1}{PrNt}\ln\left(1+PrNt\,e^{-Pr(\frac{b}{\beta}-Nb)}\theta'(0)\int_0^\eta e^{Pr[-a\sigma+\frac{b}{\beta}e^{-\beta\sigma}-Nb\,\phi(\sigma)]}d\sigma\right). \tag{11}$$

By using the boundary condition ($\theta(\infty) = 0$), we find that

$$\theta'(0) = \frac{(e^{-PrNt}-1)}{PrNt\,e^{-Pr(\frac{b}{\beta}-Nb)}}\left[\int_0^\infty e^{Pr[-a\sigma+\frac{b}{\beta}e^{-\beta\sigma}-Nb\,\phi(\sigma)]}d\sigma\right]^{-1}. \tag{12}$$

On using (12) into (11), yields

$$\theta(\eta) = 1+\frac{1}{PrNt}\ln\left[1+(e^{-PrNt}-1)\frac{\int_0^\eta e^{Pr[-a\sigma+\frac{b}{\beta}e^{-\beta\sigma}-Nb\,\phi(\sigma)]}d\sigma}{\int_0^\infty e^{Pr[-a\sigma+\frac{b}{\beta}e^{-\beta\sigma}-Nb\,\phi(\sigma)]}d\sigma}\right]. \tag{13}$$

This explicit relation for $\theta(\eta)$ in terms of $\phi(\eta)$ shall be used in subsequent Sections to derive the exact solutions at particular values of the permanent parameters in which the involved integrals can be evaluated analytically. In addition, Eq. (9) is also solved for $\phi'(\eta)$ as a 1st-order ordinary differential equation (ODE) and thus

$$\phi'(\eta) = e^{-\frac{Le\,b}{\beta}}\phi'(0)\,e^{-Le(a\eta-\frac{b}{\beta}e^{-\beta\eta})} - \frac{Nt}{Nb}e^{-Le(a\eta-\frac{b}{\beta}e^{-\beta\eta})}\int_0^\eta e^{Le(a\xi-\frac{b}{\beta}e^{-\beta\xi})}\theta''(\xi)d\xi. \tag{14}$$

By integrating Eq. (14) once again with respect to η, where $\phi(0) = 1$, we have

$$\begin{aligned}\phi(\eta) = 1+e^{-\frac{Le\,b}{\beta}}\phi'(0)\int_0^\eta e^{-Le(a\sigma-\frac{b}{\beta}e^{-\beta\sigma})}d\sigma \\ -\frac{Nt}{Nb}\int_0^\eta e^{-Le(a\sigma-\frac{b}{\beta}e^{-\beta\sigma})}\int_0^\sigma e^{Le(a\xi-\frac{b}{\beta}e^{-\beta\xi})}\theta''(\xi)d\xi d\sigma.\end{aligned} \tag{15}$$

The condition at infinity ($\phi(\infty) = 0$) leads to

$$e^{-\frac{Le\,b}{\beta}}\phi'(0) = \left(-1 + \frac{Nt}{Nb}\int_0^{\infty} e^{-Le(a\sigma - \frac{b}{\beta}e^{-\beta\sigma})} \int_0^{\sigma} e^{Le(a\xi - \frac{b}{\beta}e^{-\beta\xi})}\theta''(\xi)d\xi d\sigma \right) \Bigg/ \left(\int_0^{\infty} e^{-Le(a\sigma - \frac{b}{\beta}e^{-\beta\sigma})} d\sigma \right). \tag{16}$$

Therefore, $\phi(\eta)$ in Eq. (15) becomes

$$\phi(\eta) = 1 + \frac{\int_0^{\eta} e^{-Le(a\sigma - \frac{b}{\beta}e^{-\beta\sigma})} d\sigma}{\int_0^{\infty} e^{-Le(a\sigma - \frac{b}{\beta}e^{-\beta\sigma})} d\sigma} \left(-1 + \frac{Nt}{Nb}\int_0^{\infty} e^{-Le(a\sigma - \frac{b}{\beta}e^{-\beta\sigma})} \int_0^{\sigma} e^{Le(a\xi - \frac{b}{\beta}e^{-\beta\xi})}\theta''(\xi)d\xi d\sigma \right)$$

$$- \frac{Nt}{Nb}\int_0^{\eta} e^{-Le(a\sigma - \frac{b}{\beta}e^{-\beta\sigma})} \int_0^{\sigma} e^{Le(a\xi - \frac{b}{\beta}e^{-\beta\xi})}\theta''(\xi)d\xi d\sigma. \tag{17}$$

3. EXACT SOLUTION AT $Nt = 0$ AND $Nb = 0$

In this Section, we discuss the possibility of deriving exact solutions for the current physical problem at $Nt = 0$, $Nb = 0$. Also, comparisons with the results in the literature are to be introduced. Setting $Nb = 0$ into Eq. (13) and then taking the limit as $Nt \to 0$, we obtain $\theta(\eta)$ is a simpler closed form expression as

$$\theta(\eta) = 1 - \frac{\int_0^{\eta} e^{Pr\left[-a\sigma + \frac{b}{\beta}e^{-\beta\sigma}\right]} d\sigma}{\int_0^{\infty} e^{Pr\left[-a\sigma + \frac{b}{\beta}e^{-\beta\sigma}\right]} d\sigma}, \tag{18}$$

where β is the solution of Eq. (7). Following [16], we have

$$\int_0^{\eta} e^{Pr\left[-a\sigma + \frac{b}{\beta}e^{-\beta\sigma}\right]} d\sigma = \frac{1}{\beta}\left(\frac{-\beta}{b\,Pr}\right)^{\frac{a\,Pr}{\beta}} \Gamma\left(\frac{a\,Pr}{\beta}, -\frac{b\,Pr}{\beta}e^{-\beta\eta}, -\frac{b\,Pr}{\beta}\right), \tag{19}$$

where $\Gamma(a, z_0, z_1)$ is the generalized Gamma function. On using the result of (20) as $\eta \to \infty$, we have

$$\int_0^{\infty} e^{Pr\left[-a\sigma+\frac{b}{\beta}e^{-\beta\sigma}\right]}d\sigma = \frac{1}{\beta}\left(\frac{-\beta}{b\,Pr}\right)^{\frac{a\,Pr}{\beta}}\Gamma\left(\frac{a\,Pr}{\beta},0,-\frac{b\,Pr}{\beta}\right). \tag{20}$$

Accordingly, an exact solution for $\theta(\eta)$ is obtained as

$$\theta(\eta) = 1-\frac{\Gamma\left(\frac{a\,Pr}{\beta},-\frac{b\,Pr}{\beta}e^{-\beta\eta},-\frac{b\,Pr}{\beta}\right)}{\Gamma\left(\frac{a\,Pr}{\beta},0,-\frac{b\,Pr}{\beta}\right)} = \frac{\Gamma\left(\frac{a\,Pr}{\beta},0,-\frac{b\,Pr}{\beta}e^{-\beta\eta}\right)}{\Gamma\left(\frac{a\,Pr}{\beta},0,-\frac{b\,Pr}{\beta}\right)}. \tag{21}$$

4. APPLICATION OF ADM

The possibility of applying Adomian's method to obtain the approximate solutions for the governing equations is the subject of this Section. According to Adomian's method, the solutions are assumed in a decomposition series form as

$$\theta(\eta) = \sum_{n=0}^{\infty}\theta_n(\eta), \quad \phi(\eta) = \sum_{n=0}^{\infty}\phi_n(\eta). \tag{22}$$

It is important to note that the second term on the right hand side of Eq. (13) is a nonlinear term in ϕ, which can be decomposed into a series of Adomian's polynomials A_n as

$$\ln\left[1+(e^{-PrNt}-1)\frac{\int_0^{\eta} e^{Pr[-a\sigma+\frac{b}{\beta}e^{-\beta\sigma}-Nb\,\phi(\sigma)]}d\sigma}{\int_0^{\infty} e^{Pr[-a\sigma+\frac{b}{\beta}e^{-\beta\sigma}-Nb\,\phi(\sigma)]}d\sigma}\right] = \sum_{n=0}^{\infty}A_n, \tag{23}$$

where these A_n are defined by

$$A_n = \frac{1}{n!}\frac{d^n}{d\lambda^n}\ln\left[1+(e^{-PrNt}-1)\frac{\int_0^{\eta} e^{Pr[-a\sigma+\frac{b}{\beta}e^{-\beta\sigma}-Nb\,\phi(\sigma)]}d\sigma}{\int_0^{\infty} e^{Pr[-a\sigma+\frac{b}{\beta}e^{-\beta\sigma}-Nb\,\phi(\sigma)]}d\sigma}\right]_{\lambda=0}. \tag{24}$$

Inserting (23) and (24) into (13) and (17) and applying Adomian's method, we can

then set the following system of two-coupled recurrence schemes for $\theta(\eta)$ and $\phi(\eta)$ as

$$\theta_0(\eta) = 1, \tag{25}$$

$$\theta_{n+1}(\eta) = \frac{1}{NtPr} A_n, \tag{26}$$

$$\phi_0(\eta) = 1 - \frac{\int_0^{\eta} e^{-Le(a\sigma - \frac{b}{\beta}e^{-\beta\sigma})} d\sigma}{\int_0^{\infty} e^{-Le(a\sigma - \frac{b}{\beta}e^{-\beta\sigma})} d\sigma}, \tag{27}$$

$$\phi_{n+1}(\eta) = \frac{Nt}{Nb}\int_0^{\infty} e^{-Le(a\sigma - \frac{b}{\beta}e^{-\beta\sigma})} \int_0^{\sigma} e^{Le(a\xi - \frac{b}{\beta}e^{-\beta\xi})} \theta''(\xi) d\xi d\sigma -$$

$$\frac{Nt}{Nb}\int_0^{\eta} e^{-Le(a\sigma - \frac{b}{\beta}e^{-\beta\sigma})} \int_0^{\sigma} e^{Le(a\xi - \frac{b}{\beta}e^{-\beta\xi})} \theta''(\xi) d\xi d\sigma, \quad n \geq 0. \tag{28}$$

The recurrence scheme for $\phi(\eta)$ can be also simplified and written as

$$\phi_0(\eta) = \frac{\Gamma\left(\frac{a\,Le}{\beta}, 0, -\frac{b\,Le}{\beta} e^{-\beta\eta}\right)}{\Gamma\left(\frac{a\,Le}{\beta}, 0, -\frac{b\,Le}{\beta}\right)}, \tag{29}$$

$$\phi_{n+1}(\eta) = \frac{Nt}{Nb}\left[(1-\phi_0) I_n(\infty) - I_n(\eta)\right], \tag{30}$$

where $I_n(\eta)$ and $I_n(\infty)$ are given by

$$I_n(\eta) = \int_0^{\eta} e^{-Le(a\sigma - \frac{b}{\beta}e^{-\beta\sigma})} \int_0^{\sigma} e^{Le(a\xi - \frac{b}{\beta}e^{-\beta\xi})} \theta''(\xi) d\xi d\sigma, \tag{31}$$

and

$$I_n(\infty) = \int_0^{\infty} e^{-Le(a\sigma - \frac{b}{\beta}e^{-\beta\sigma})} \int_0^{\sigma} e^{Le(a\xi - \frac{b}{\beta}e^{-\beta\xi})} \theta''(\xi) d\xi d\sigma. \tag{32}$$

5. RESULTS AND DISCUSSION

5.1. STRETCHING SHEET AND NUMERICAL VALIDATION

This Subsection is devoted to compare between the present results and the corresponding results in the literature at the same values of the selected parameters.

5.1.1. AT $\lambda = s = 0$

In Table 1, comparisons of the present exact numerical results for $(-\theta'(0))$ at different values of Pr when $Nt = 0$, $Nb = 0$, $\lambda = 0$, and $s = 0$ with those obtained in Refs. [11, 37–39] are presented. In this case, we have from (7) that $\beta = 1$ for the stretching sheet. Therefore, the exact solution (21) is used here with $a = 1$ and $b = -1$ to conduct the numerical results in Table 1 for $(-\theta'(0))$, where

$$\theta(\eta) = \frac{\Gamma(Pr, 0, Pr\, e^{-\eta})}{\Gamma(Pr, 0, Pr)}, \tag{33}$$

and

$$-\theta'(0) = \frac{(Pr)^{Pr} e^{-Pr}}{\Gamma(Pr, 0, Pr)}. \tag{34}$$

It is shown from Table 1 that the results in the literature coincide with the present numerical values in most cases. However, the value of $(-\theta'(0))$ obtained in [11] by using the homotopy analysis method when $Pr = 0.7$ may be not accurate enough, where it agrees with the current exact value up to only two decimal places. In addition, the calculated value obtained in [40] may need some revisions because it was completely different than the current exact value and also than those in Refs. [11], [37], and [38].

Table 1

Comparison of results for $(-\theta'(0))$ at $s = 0$, $\lambda = 0$, $Nt = 0$, $Nb = 0$.

Pr	Khan and Pop [37]	Wang [38]	Gorla and Sidawi [39]	Hassani *et al*. [11]	Present results
0.07	0.0663	0.0656	0.0656	-	0.0655625
0.20	0.1691	0.1691	0.1691	0.1692	0.169089
0.70	0.4539	0.4539	0.5349	0.4582	0.453916
2.00	0.9113	0.9114	0.9114	0.9114	0.911358
7.00	1.8954	1.8954	1.8905	1.8956	1.895403
20.00	3.3539	3.3539	3.3539	3.3539	3.353904
70.00	6.4621	6.4622	6.4622	6.4623	6.462199

5.1.2. AT $\lambda \neq 0, s = 0$

In this case, we have

$$-f''(0) = -\beta^2 b, \quad b = -\frac{1}{\lambda\beta^2 + \beta}, \tag{35}$$

where β is the positive real root for the following cubic equation

$$\lambda\beta^3 + \beta^2 - 1 = 0. \tag{36}$$

The values of the skin friction $(-f''(0))$ are calculated by using the exact solution given by Eqs. (6-7) and compared in Table 2 with those obtained in [13] and [23] by using the homotopy analysis method at different values of λ. In view of the current exact solution for the f -equation, it can be concluded from Table 2 that the present results of the skin friction $(-f''(0))$ agree with those obtained by Noghrehabadi *et al*. [13] and by Mabood *et al*. [23] up to five or six decimal places. On the other hand, to stand on the accuracy of Adomian's method, the present algorithm given by Eqs. (25-28) are used to conduct several numerical results for $(-\theta'(0))$ and $(-\phi'(0))$ by using only two terms. These approximate solutions are then compared with the available results in the literature at various values of λ, Nt, and Nb when $Pr = Le = \nu = 10$ in the absence of the suction parameter, *i.e*., at $s = 0$. It can be seen from Table 3 that the current numerical results obtained by the present ADM are in full agreement with those obtained in [13] and [23] by using the homotopy analysis method.

We conclude that the current two-term approximate solution of Adomian's method achieved the same accuracy of the homotopy analysis method using 40 terms of the homotopy series.

Table 2

Comparison of results for $(-f''(0))$ at different values for λ at $s = 0$.

λ	Noghrehabadi *et al*. [13]	Mabood *et al*. [23]	Present results
0.1	0.872082	0.872082	0.87208247
0.3	0.701548	0.701548	0.70154821
0.5	0.591195	0.591195	0.59119548
1.0	0.430160	0.430160	0.43015971
2.0	0.283980	0.283981	0.28397959
5.0	0.144841	0.144843	0.14484019
10.	0.081243	0.081246	0.08124198

Table 3

Comparison of results for $(-\theta'(0))$ and $(-\phi'(0))$ at $s = 0, \nu = Le = \Pr = 10$.

λ	*Nb*	*Nt*	$(-\theta'(0))$			$(-\phi'(0))$		
			[13]	H A M [23]	Present results	[13]	H A M [23]	Present results
0.5	0.2	0.1	0.424328	0.424328	0.42432776	1.999070	1.999072	1.99907252
		0.2	0.306640	0.306640	0.30664021	2.110990	2.110993	2.11099348
		0.3	0.229206	0.229207	0.22920659	2.228691	2.228691	2.22869197
1.0	0.3	0.1	0.190347	0.190346	0.19034699	1.819268	1.819267	1.81926938
		0.2	0.137084	0.137084	0.13708403	1.898513	1.898513	1.89851463
		0.3	0.102297	0.102297	0.10229664	1.969337	1.969337	1.96933898

5.2. SHRINKING SHEET AND DUAL SOLUTION

In this Subsection, we begin with illustrating the possibility of obtaining the dual solution of the temperature and the fluid velocity. In the next Subsection, we focus on the dual solution of the temperature, where the exact expression of the temperature is available from Eq. (21) at a special case, *i.e.*, at $Nt = Nb = 0$. While in the later Subsection, we consider the approximate dual solutions of both the temperature, the concentration, and the fluid velocity in the general case.

5.2.1. EXACT DUAL SOLUTION AT $Nt = Nb = 0$

On considering the case of the shrinking sheet, it follows from Eq. (6) and Eq. (21) that

$$\theta(\eta) = \frac{\Gamma\left(\frac{a\,Pr}{\beta}, 0, -\frac{b\,Pr}{\beta}e^{-\beta\eta}\right)}{\Gamma\left(\frac{a\,Pr}{\beta}, 0, -\frac{b\,Pr}{\beta}\right)}, \quad a = s - \frac{1}{\lambda\beta^2+\beta}, \quad b = \frac{1}{\lambda\beta^2+\beta}, \tag{37}$$

where β is at least two positive real values for the following cubic equation

$$\lambda\beta^3 + (1-\lambda s)\beta^2 - s\beta + 1 = 0. \tag{38}$$

In Figs. (1-3), the effects of s, λ, and Pr on the temperature are depicted. Figure 1 shows that there is a dual solution for θ that decreases with increasing s. However, at the lowest value of the suction parameter, *i.e.*, at $s = 1$, the upper and the lower branch of the dual solution are nearly identical. This is because the two

positive values of β (the two positive roots of Eq. (38)) are close to each other. The effects of λ on the variation of θ is shown in Fig. 2, where two different behaviors have been detected for the temperature. It is clear from this figure that the upper branch is increased by increasing the slip parameter while a converse behavior has been found for the lower branch.

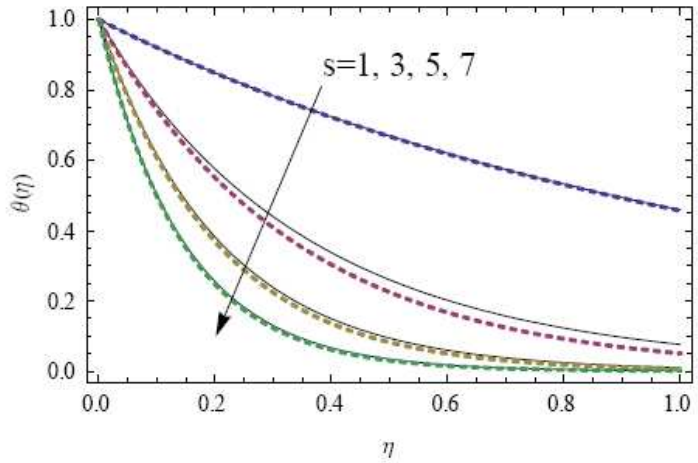

Fig. 1. The dual solution of temperature at various values of s for $\lambda = 5.22$, $\Pr = 1$, $Nb = Nt = 0$.

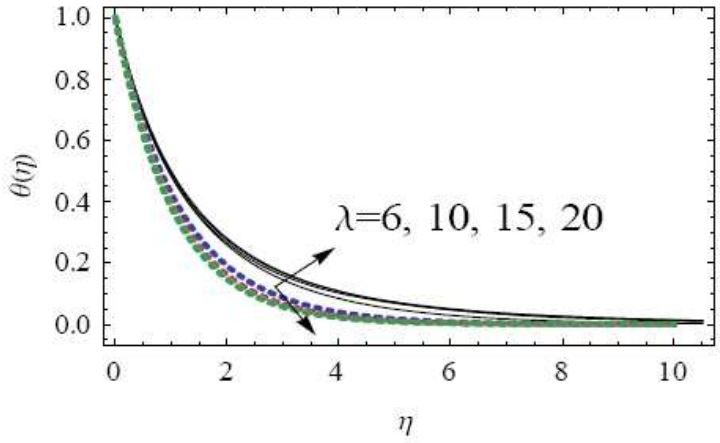

Fig. 2. The dual solution of temperature at various values of λ for $s = 1$, $\Pr = 1$, $Nb = Nt = 0$.

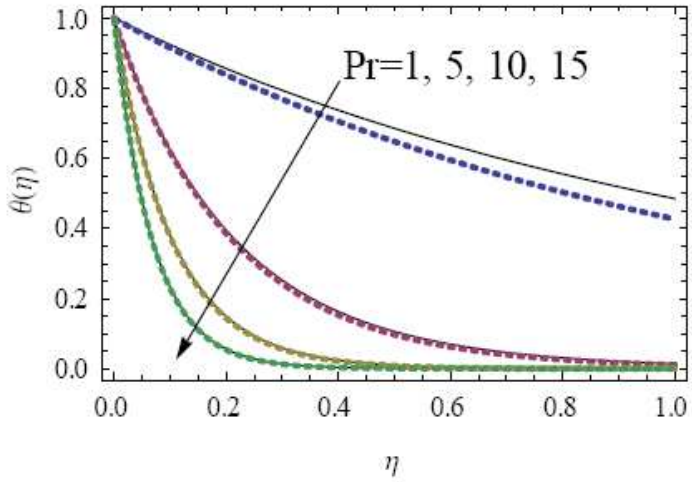

Fig. 3. The dual solution of temperature at various values of Pr for $s = 1, \lambda = 6, Nb = Nt = 0$.

Figure 3 indicates that the dual temperature profile is decreased by increasing the Prandtl number Pr. It is also observed from this figure that the two branches of the dual temperature solution are nearly identical at higher value of the Prandtl number.

5.2.2. APPROXIMATE DUAL SOLUTION AT $Nt \neq 0, Nb \neq 0$

In this Subsection, the two-term Adomian approximate solution has been used to study the effects of Le, s, λ, Nt, and Nb on the dual solutions of the temperature, the concentration, and the fluid velocity.

Figure 4 indicates the effect of Lewis number Le on the dual nano-particle concentration ϕ. It is clear that ϕ is decreased by increasing Le. This behavior occurs for both of the dual upper and lower branches. It should be mentioned here that the behavior of ϕ in Fig. 4 is the same as in the stretching sheet that has been considered in [16], Fig. 7, when $s = 0$.

The effect of Lewis number Le on the dual temperature is depicted in Fig. 5. It is observed from this figure that the increase in Le increases the dual temperature. The effect of the suction parameter s on the dual velocity profile is displayed in Fig. 6. As shown from this figure, increasing s leads to decreasing $f'(\eta)$ in the whole domain for the lower branch of the dual solution. However, $f'(\eta)$ decreases with increasing s in a certain domain of the upper branch and then a converse behavior has been observed in the rest of the domain.

The effect of the slip parameter λ on the dual velocity is plotted in Fig. 7. It is found that the upper and the lower branch decrease with increasing λ.

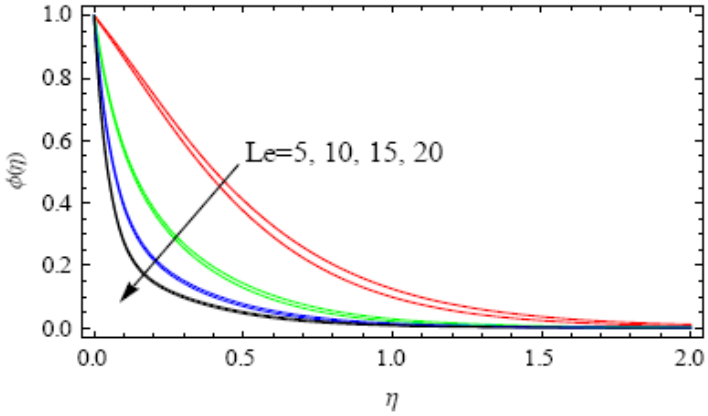

Fig. 4. The effect of Lewis number on dual conentration at $s = 1, \lambda = 6, \Pr = 5, Nb = Nt = 0.1$.

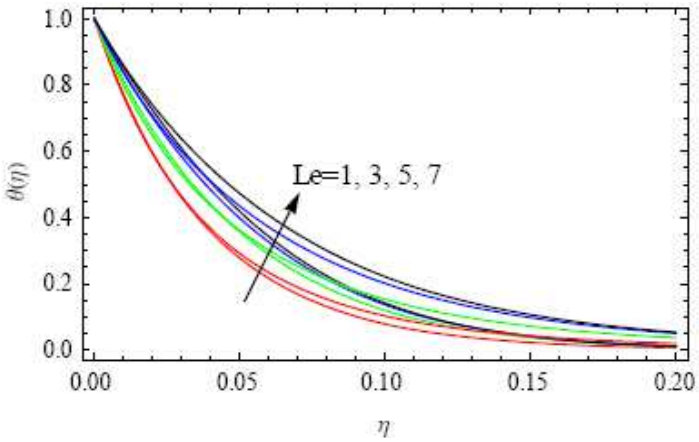

Fig. 5. The effect of Lewis number on dual temperature at $s = 3, \lambda = 1, \Pr = 10, Nb = Nt = 0.1$.

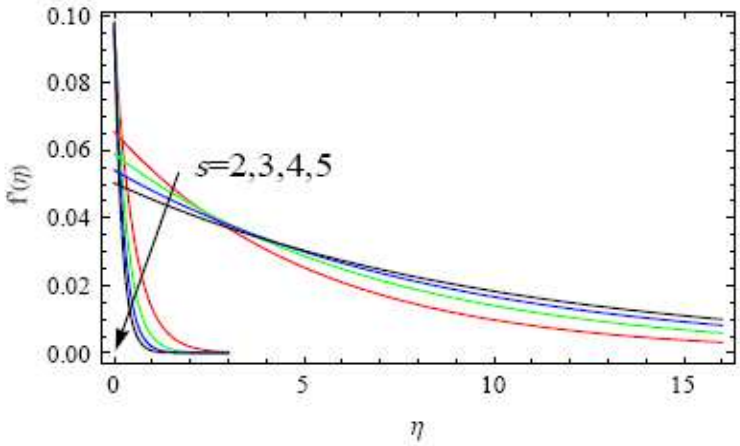

Fig. 6. The effect of suction parameter on dual velocity at $\lambda = 10$.

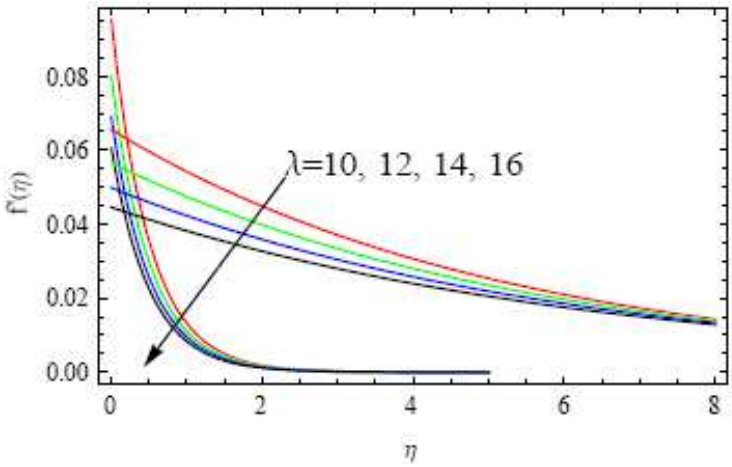

Fig. 7. The effect of slip parameter on dual velocity at $s = 2$.

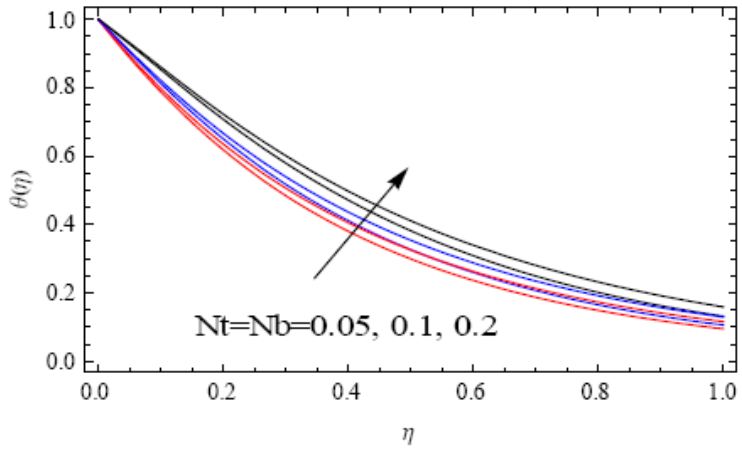

Fig. 8. The effect of Nb, Nt on dual tempaerature at $s = 1$, $\lambda = 6$, Pr = 3, $Le = 10$.

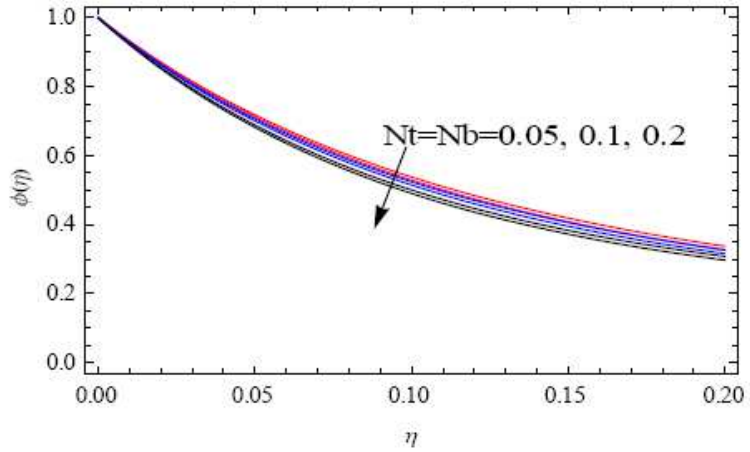

Fig. 9. The effect of Nb, Nt on dual concentration at $s = 1$, $\lambda = 6$, Pr = 3, $Le = 10$.

This discussion is ended with the effects of both Nt and Nb on the dual solutions of the temperature and the concentration in Fig. 8 and Fig. 9, respectively. As usual, the increase in both Nt and Nb increases the temperature for both branches as in Fig. 8, while the increase in both Nt and Nb decreases the concentration for both branches as in Fig. 9.

6. CONCLUSIONS

The boundary layer nanofluid flow and heat transfer over a stretching/shrinking sheet have been investigated in the present research by considering the effects of the suction and the slip parameters. For stretching sheet, some differences were found between the current exact results for the Nusselt number (in the absence of some parameters) and those in the literature. In addition, the present exact results of the skin friction agree with those obtained [13, 23] up to five or six decimal places at various values of the slip parameter and no suction. Also, the numerical results obtained by the present ADM for Nusselt and Shroder numbers are in full agreement with those obtained in [13, 23] by using the homotopy analysis method. Moreover, the exact dual solution is obtained in the case of shrinking sheet in a special case, while the approximate dual solution has been obtained in the general case by Adomian's method. Finally, several plots have been given for the effects of various parameters on the dual velocity, the dual temperature, and the dual nano-particle concentration.

Acknowledgments. This Project was funded by the Deanship of Scientific Research (DSR) at King Abdulaziz University, Jeddah, under grant no. G-563-363-38. The authors, therefore, acknowledge with thanks DSR for technical and financial support.

REFERENCES

1. G. Adomian, *Solving Frontier Problems of Physics: The Decomposition Method*, Kluwer Academic, Boston, 1994.
2. A.M. Wazwaz, Appl. Math. Comput. **166**, 652–663 (2005).
3. N.T. Eldabe *et al.*, Phys. Lett. A, **363**, 257–259 (2007).
4. A.M. Wazwaz, Appl. Math. Comput. **216**, 1304–1309 (2010).
5. A. Ebaid, Z. Naturforschung A **66**, 423–426 (2011).
6. J.S. Duan and R. Rach, Appl. Math. Comput. **218**, 4090–4118 (2011).
7. A. Ebaid, J. Comput. Appl. Math., **235**, 1914–1924 (2011).
8. A. Alshaery and A. Ebaid, Acta Astronautica **140**, 27–33 (2017).
9. A. Ebaid, Computational and Mathematical Methods in Medicine **2013**, 547954 (2013).
10. H.O. Bakodah *et al.*, Rom. Rep. Phys. **70**, XYZ (2018).
11. M. Hassani *et al*., Int. J. Therm. Sci. **50**, 2256–2263 (2011).
12. A.A. Gaber and A. Ebaid, Rom. Rep. Phys. **70**, XYZ (2018).
13. A. Noghrehabadi, R. Pourrajab, M. Ghalambaz, Int. J. Therm. Sci. **54**, 253–261 (2012).
14. A. Ebaid *et al.*, Advances in Mathematical Physics **2014**, 538950 (2014).
15. A. Ebaid and M.A. Al Sharif, Zeitschrift für Naturforschung A **70** (6), 471–475 (2015).
16. F. Mabood *et al.*, Journal of Magnetism and Magnetic Materials **374**, 569–576 (2015).
17. J.P. Boyd, Computers in Physics **11**(3), 299–303 (1997).
18. A.M. Wazwaz, Appl. Math. Comput. **105**(1), 11–19 (1999).
19. A.M. Wazwaz, Appl. Math. Comput. **182**(2), 1812–1818 (2006).

20. A.M. Wazwaz, Appl. Math. Comput. **182**(2), 1812–1818 (2006).
21. A. Ebaid *et al.*, Applied Mathematics Letters **46**, 117–122 (2015).
22. N. Ishfaq *et al.*, Journal of Hydrodynamics **28**(4), 596-602 (2016).
23. F. Mabood *et al.*, Thermal Science **21**(1A), 289–301 (2017).
24. H. Leblond, H. Triki, and D. Mihalache, Phys. Rev. A **85**, 053826 (2012).
25. D. Mihalache, Rom. J. Phys. **59**, 295–312 (2014).
26. D. Mihalache, Proc. Romanian Acad. A **16**, 62– 69 (2015).
27. A.M. Wazwaz, Rom. J. Phys. **60**, 56–71 (2015).
28. A.M. Wazwaz, Rom. J. Phys. **61**, 774–783 (2016).
29. A.M. Wazwaz *et al*., Rom. Rep. Phys. **69**, 102 (2017).
30. Y. Zhang, D. Baleanu, and X.J. Yang, Proc. Romanian Acad. A **17**, 230–236 (2016).
31. I.A. Cristescu, Rom. Rep. Phys. **68**, 962–978 (2016).
32. R.M. Hafez *et al*., Rom. Rep. Phys. **68**, 112–127 (2016).
33. L. Bougoffa, Rom. J. Phys. **62**, 110 (2017).
34. A.M. Wazwaz *et al*., Rom. Rep. Phys. **69**, 102 (2017).
35. I.A. Cristescu, Rom. Rep. Phys. **68**, 473–485 (2016).
36. D. Mihalache, Rom. Rep. Phys. **69**, 403 (2017).
37. W.A. Khan and I. Pop, Int. J. Heat Mass Transfer **53**, 2477–2483 (2010).
38. C.Y. Wang, J. Appl. Math. Mech. (ZAMM) **69** , 418–420 (1989).
39. R.S.R. Gorla and I. Sidawi, Appl. Sci. Res. **52**, 247–257 (1994).